Predicting rainfall in the Dutch Caribbean — more than El Niño?

Albert Martis*
Geert Jan van Oldenborgh and Gerrit Burgers§

June 21, 2002

Abstract
A strong lagged relationship between ENSO and rainfall in the main rain season (Oct–Jan) on the leeward islands of Aruba, Curaçao and Bonaire is found. It can easily be used for skillful seasonal predictions, with an anomaly correlation coefficient $r \approx 0.6$ at lag 4 months on historical data. The other two seasons, Feb–May and Jun–Sep, also show correlations with ENSO that can be exploited for predictions, $r = 0.4$ to 0.5. In the Feb–May dry season there is also a lagged correlation with sea surface temperature in the Pacific Ocean off the Central American coast that can be used to increase the forecast skill. A Jun–Sep small rains season correlation to equatorial Atlantic Ocean SST is absent in earlier data. Most of these results are also applicable to other stations in northern South America. Regressions with the circulation show that the main intermediate factors are upper-level divergence and vorticity, and at lower levels a veering of the trade winds. This modifies the descending limb of the sea-continent breeze circulation that is responsible for the dry zone off the coast.

1 Introduction

The leeward islands of the Dutch Caribbean, Aruba, Curaçao and Bonaire, lie in the Caribbean Sea off the coast of Venezuela, around 12°N, 68–70°W. They have a semi-arid climate, with an annual precipitation of around 550mm. The year-to-year variations are large: the standard deviation is larger than the mean. In this paper the predictability of these variations is investigated. Due to the high price of water on these densely populated islands, predictions of the seasonal precipitation with lead times of a few months would be welcome.

* Meteorological Service Netherlands Antilles, Seru Mahuma z/n, Curaçao
§ KNMI, P. O. Box 201, NL-3730 AE De Bilt, The Netherlands

There are well-established El Niño–Southern Oscillation (ENSO) teleconnections to northern South America (e.g., Ropelewski and Halpert, 1987; Kiladis and Diaz, 1989) with extensions to the Caribbean region (Enfield and Alfaro, 1999). Variations in precipitation in the Caribbean have also been linked to simultaneous subtropical and tropical Atlantic Ocean sea surface temperature anomalies Hastenrath (1984); Enfield and Alfaro (1999); Giannini *et al.* (2000). However, the climatology of the islands along the Venezuelan coast is quite different from the normal Caribbean climate. Besides being much drier, the main rain season is in the winter (Oct–Jan), whereas in most of the region it falls in summer (May-Oct).

The main subject of this paper is the predictability of the rainfall on the leewards islands of the Dutch Caribbean. As it forms the basis for an operational forecast system, the lag structure of the correlations is an important factor. The region is not mentioned in the review of Hastenrath (1995), which also has this focus.

The layout of this article is as follows. First the climatology of the islands is discussed. Next the seasonal predictability is investigated for a single station for all seasons. This is the quantity of interest to most users. The resulting statistical models are verified against other stations with non-overlapping years of data. Next island averages are considered, using all available station data. These may have different characteristics than single-station correlations. The regional extend of the teleconnections is also noted. Conclusions are drawn to the suitability of the results for operational seasonal forecasting.

2 Climatology

The leeward islands of the Dutch Antilles (Aruba, Curaçao and Bonaire) have a semi-arid climate (yearly precipitation is about 550mm per year). This is due to an extension of the Azores high and locally it is also connected with an upwelling zone with colder sea surface temperature (SST) along the east-west Venezuelan coast caused by the easterly trade winds (Lahey, 1958; Trewartha, 1981). The influence of the mainland 60km away is large: during the rain season most precipitation is late at night and in the early morning, opposite to the usual tropical pattern, which exists on the mainland. This is caused by the sea-continent breeze.

Except the western-most part of Curaçao (elevation 375m) the islands are quite flat, with hills lower than 100m. Most precipitation is in the form of convective events. These are very local: monthly means can differ by up to a factor two for stations that are just 10km apart.

The main station used is Hato Airport at Curaçao on the north coast, 12.20°N, 69.00°W, elevation 8m. Data from 1951 to 1996 with 7 missing months was retrieved from the GHCN database (Vose *et al.*, 1992). The seasonal cycle,

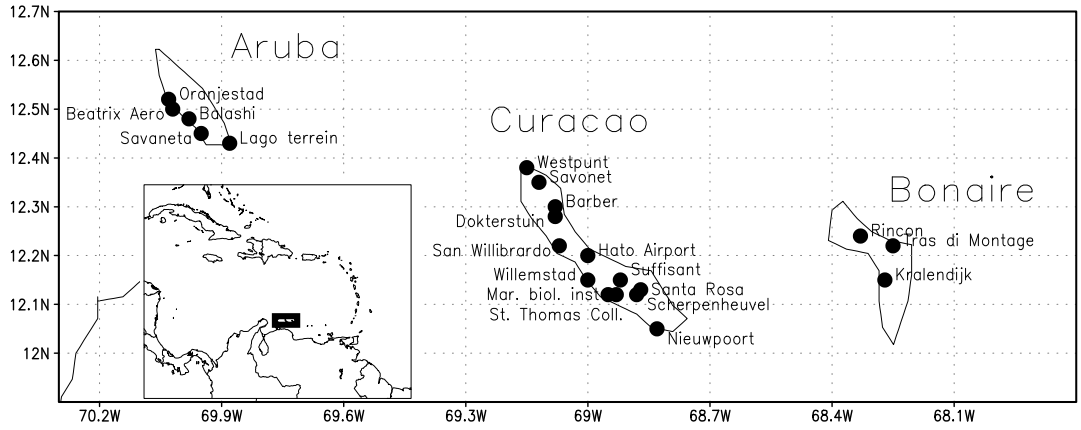

Figure 1: Map of the stations on the leeward islands with precipitation data in the GHCN v2beta database. The insert shows the location of the region in the Caribbean.

which is representative for all three islands, is shown in Fig. 2. Aruba is somewhat drier. Traditionally, the year is divided in three 4-month seasons. Oct–Jan is the rain season, Feb–May the dry season and Jun–Sep bring the small rains. The variability of the rain is high: the standard deviation is as large as the mean in most months.

Note that both the seasonal cycle and the total amount of precipitation differ greatly from the typical Caribbean pattern, which has a larger yearly sum and a rain season in summer, often interrupted by a midsummer drought (Giannini *et al.*, 2000).

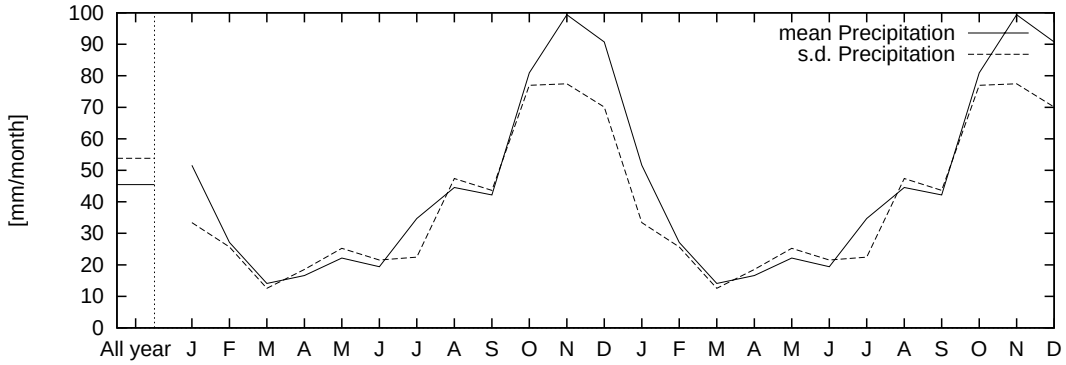

Figure 2: Seasonal cycle of rainfall at Hato Airport, Curaçao.

3 Statistical models for rainfall predictions

To establish statistical relationships the following strategy was used. First a single station is used, rather than an area average, as this is the quantity that is most relevant for many users. Hato Airport has the longest almost continuous record, 1951–1996. In this semi-arid climate the distribution of seasonal precipitation is highly skewed. However, the logarithm of precipitation (Wilks, 1995) is distributed approximately normally and has, within errors, linear relationships with predictors. First maps of (lagged) correlations between SST and the logarithm of seasonal precipitation at Hato Airport are computed, showing areas that may influence rainfall on the islands. Indices of these areas are constructed, and the resulting scatter plot inspected. Often it is found that the relationship is quite linear, and the probability density function (PDF) of the residuals (the difference between the observed logarithm of precipitation and the predicted one) does not dependent strongly on the value of the predictor. This constant PDF is then used to compute of the probability of a wet:normal:dry season as a function of the value of the predictor. The climatological probabilities are defined as 33%:33%:33%.

Next these statistical models are verified using nearly independent data at the nearby stations of Willemstad (1894–1933) and Dokterstuin (1921–1952). Area averages over the islands will be discussed in section 3.5. Unless otherwise noted, it has been checked that the results are due to interannual fluctuations by repeating the analysis with a simple year-to-year difference high-pass filter that removes longer time scale fluctuations.

3.1 Rain Season

For the Oct–Jan rain season the correlations between Hato rainfall and simultaneous SST (over sea) and T2m (over land) (Parker *et al.*, 1995; Jones, 1994; Parker *et al.*, 1994) are shown in Fig. 3. The main predictor is El Niño in the eastern Pacific. There is a positively correlated area around 35°N, 170°W ($r = 0.44^{+17}_{-13}$, the errors indicate the 95% limits -0.31 to -0.61 computed with a bootstrap method using 800 samples). However, it seems unlikely to be physically connected to the islands. This is confirmed by the absence of a correlation with independent data.

The correlation map shows that the effect of El Niño is likely due to the influence of warmer water along the Pacific coast of Central America, and in the Caribbean Sea, which forms at the later stages of an El Niño. As an index of the strength of El Niño the NINO3 index is chosen, the SST average of the area 5°S–5°N, 90°–150°W (Reynolds and Smith, 1994; Kaplan *et al.*, 1998). In Figure 4 it is shown that the highest correlations are obtained when the NINO3 index leads Hato precipitation by four months. El Niño's with a strong early onset in Jun–Sep seem to have a larger influence. This was certainly confirmed in 1997–98, when

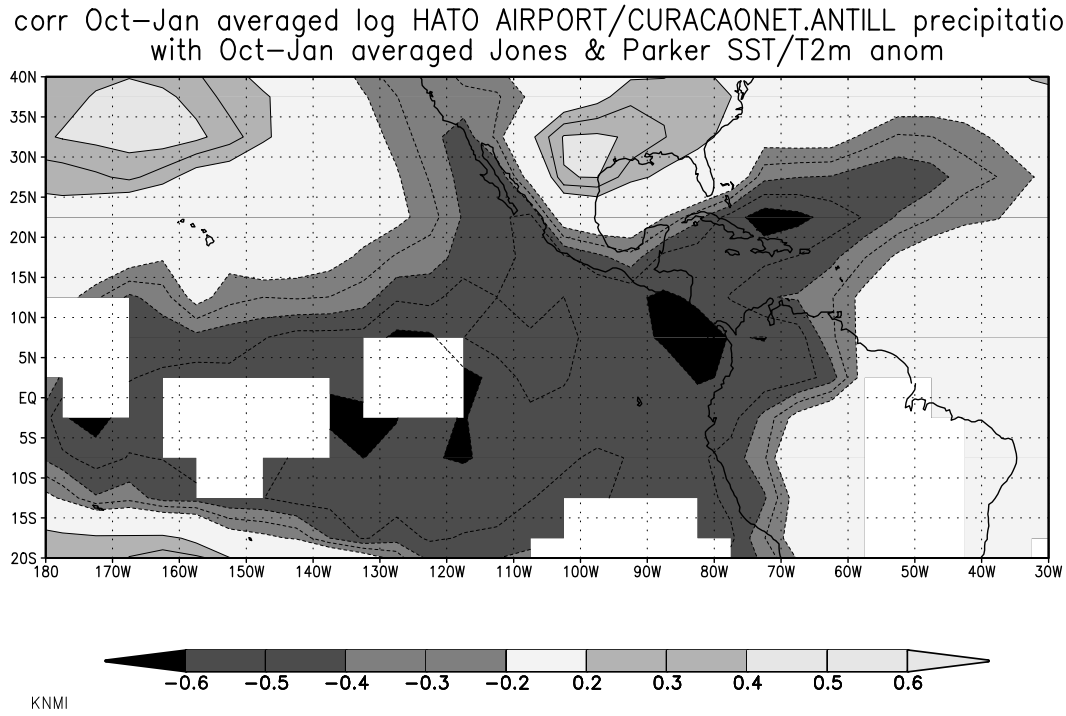

Figure 3: The correlation of the logarithm of Oct–Jan rainfall (rain season) at Hato Airport, Curaçao, with simultaneous SST/T2m. White areas indicate grid points where data is available for fewer than half the years 1951–1996.

an early and strong El Niño was followed by a severe drought, and the next two years, when the islands were dressed in luxuriant green after moderately strong La Niña's.

This relationship is in agreement with the one discussed for northern South America and the Caribbean, e.g. in Ropelewski and Halpert (1987), although the dependence on the stage of El Niño is new. The correlation coefficient between the logarithm of precipitation and the NINO3 index 4 months earlier is $r = -0.59^{+19}_{-15}$. The difference between the correlations at lag four months and no lag is not significant. The correlation is higher than most of the stations discussed in Ropelewski and Halpert (1987). In fact, it is one of the highest correlations of station precipitation data with the NINO3 index in the world. Only the areas directly affected by the shift of the convection zone from Indonesia to the Central Pacific have significantly higher values.

The scatter plot (Fig. 4c) shows that it is reasonable to assume a linear relationship between the NINO3 index and the logarithm of precipitation, although the effect of strong La Niña's seems even stronger. Assuming a probability density function of the noise around this line that is independent of ENSO, conditional

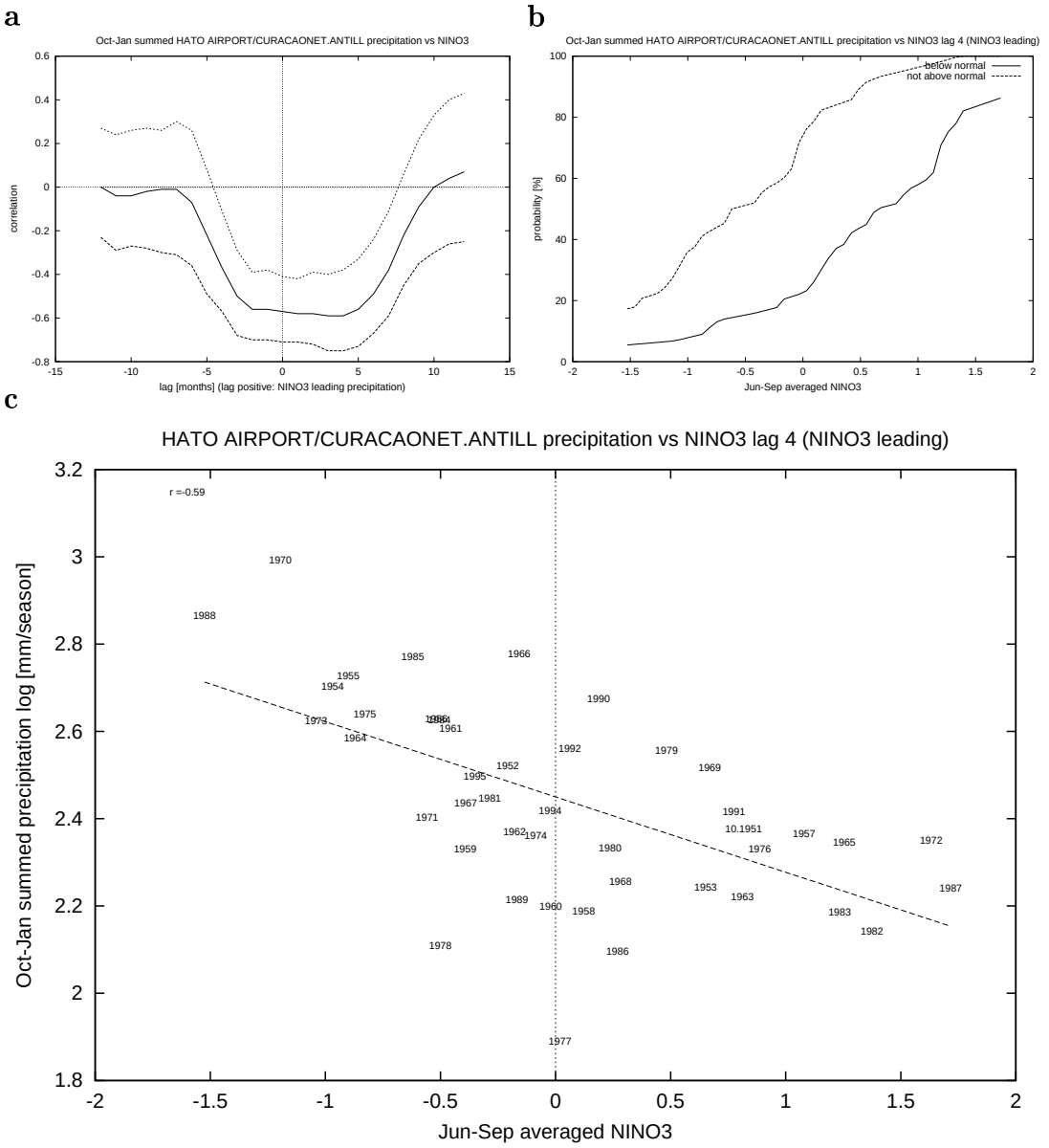

Figure 4: The correlation of the logarithm of Oct–Jan rainfall (rain season) at Hato Airport, Curaçao, with the 4-month average NINO3 index. a: lag correlations (with 95% confidence intervals), b: tercile diagram at lag 4 months, c: scatter plot at lag 4 months.

probabilities for a dry:normal:wet rain season as a function of the NINO3 index in Jun–Sep are shown in Fig. 4b. This NINO3 can be obtained before the start of the rain season from operational analyses (e.g., Reynolds and Smith, 1994). Using ENSO forecasts (e.g., Stockdale *et al.*, 1998; Ji *et al.*, 1996), which are reasonably reliable from boreal summer onwards, a seasonal forecast can be made in June.

3.2 Dry season

The dry season at Hato Airport (Feb–May) also shows significant correlations with SST four months earlier (Fig. 5). The lag correlation with the NINO3 index is $|r| \geq 0.3$ for lags 3–10 months, although with a rather large uncertainty; $r = -0.31^{+23}_{-21}$ at lag 4. A more direct measure seems to be the sea water temperature along the Pacific coast of Central America. The Kaplan SST anomalies in the region 10°–25°N, 90°–110°W are correlated with the logarithm of precipitation at Hato 4 months later with $r = -0.60^{+19}_{-15}$, and $|r| \geq 0.5$ for lags 2–6 months.

There seems to be another factor: SST in the North Atlantic. The simultaneous correlation of the logarithm of precipitation at Hato Airport with SST north of Cuba (20°–25°N, 60°–80°W) is -0.46^{+18}_{-16}. Four months earlier, there is an area of high correlations further north (25°–35°N, 60°–80°W), at $r = -0.45^{+18}_{-15}$. However, this has a large decadal component: the year-to-year differences only correlate at an insignificant $r = -0.25^{+24}_{-19}$. Also, there is no mechanism that connects this region to the more southerly area some months later. Neither persistence nor the ECMWF seasonal forecast model has great skill ($r < 0.4$) predicting SST in this area. We therefore do not consider this area further.

As predictor we therefore propose a combination of the NINO3 index and the coastal Pacific temperature, inversely weighted with their standard deviations (1 K and 0.3 K). This gives a correlation of -0.50^{+21}_{-18} at lag 4 and $|r| > 0.45$ for lags 2–7 months with the logarithm of the dry season Hato Airport precipitation. The scatter plot (Fig. 6c) again shows that the scatter seems independent of the predictor, so that the probability forecast chart Fig. 6b can be constructed.

3.3 Small rains

Finally, the small rains (Jun–Sep) are considered. The simultaneous correlations (Fig. 7) show a weak El Niño signal, a large positive correlation with tropical Atlantic SST, and a connection with the Kuroshio extension in the Northwest Pacific. It is assumed the simultaneous temperature anomalies over land will be hard to predict.

The simultaneous El Niño connection is barely significant at $r = -0.34^{+32}_{-26}$ ($P = 5\%$) and will have to be verified with independent data. For the tropical Atlantic the average SST anomaly in the area 10°S–10°N, 35°W–10°E has a correlation of $r = 0.50^{+19}_{-22}$ with the logarithm of Hato Airport precipitation. This is the

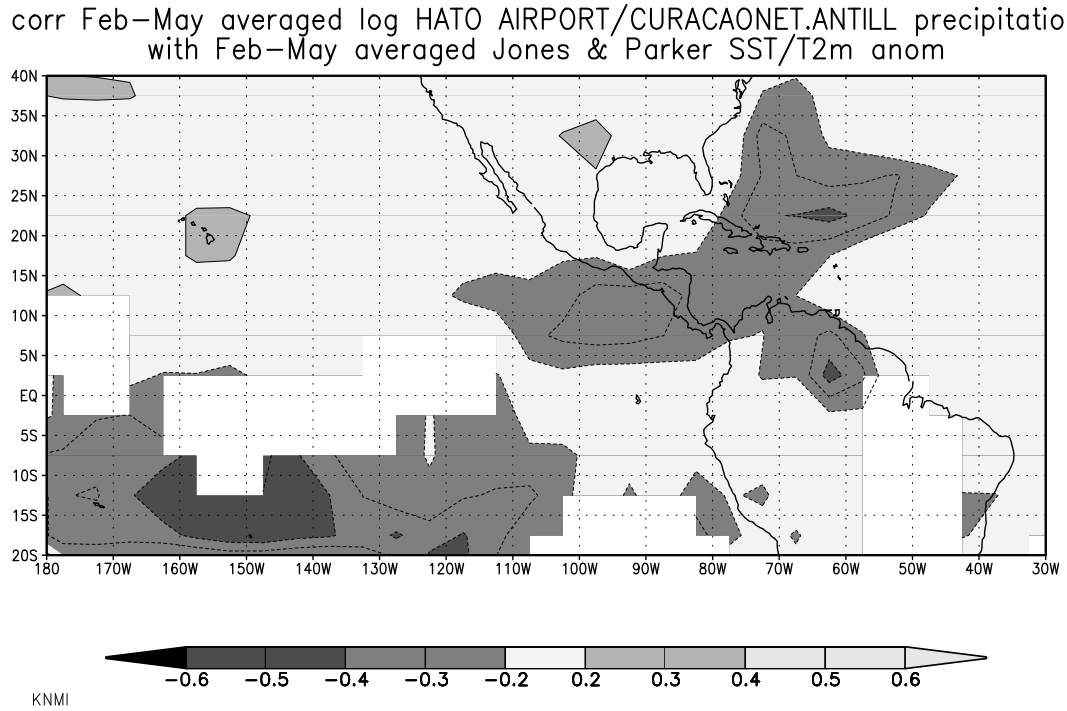

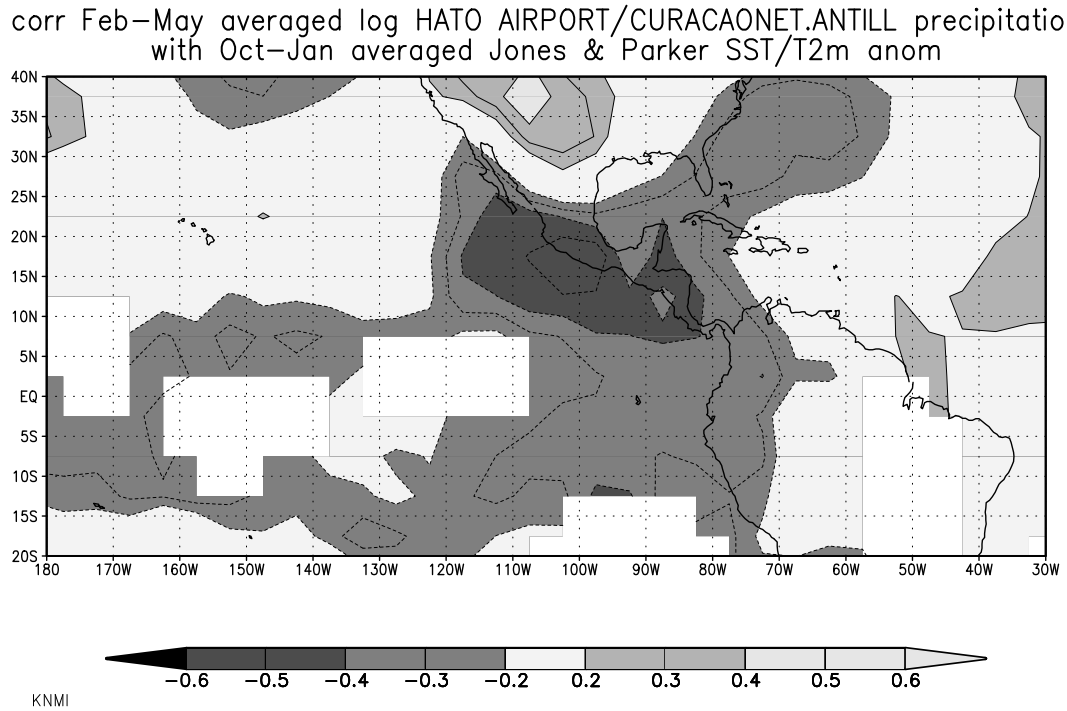

Figure 5: The correlation of Feb–May rainfall (dry season) at Hato Airport, Curaçao, with SST/T2m simultaneously (top) and four months earlier (bottom).

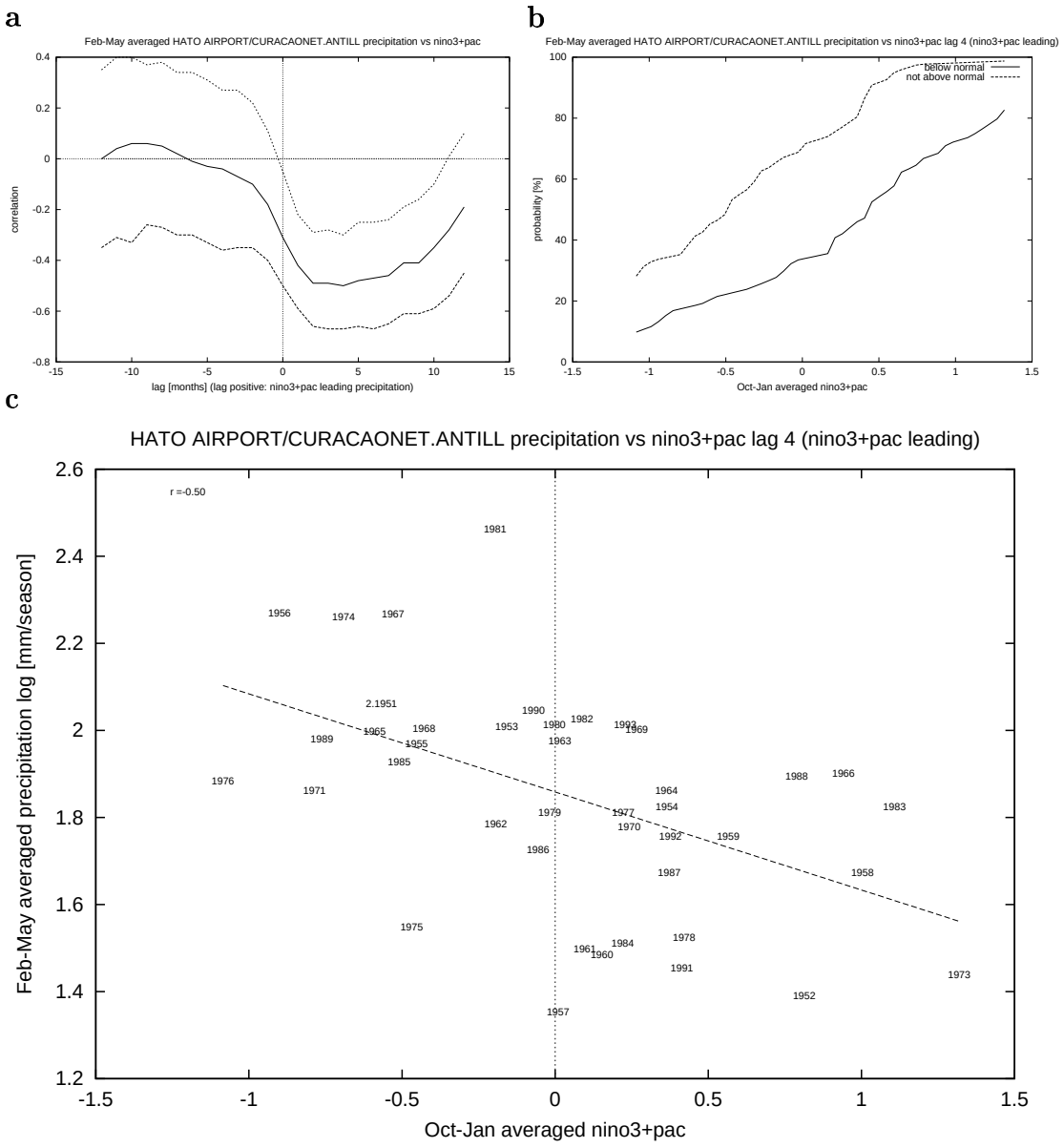

Figure 6: The correlation of the logarithm of Feb–May rainfall (dry season) at Hato Airport, Curaçao, with a combined index of NINO3 and Pacific Coast SST. a: lag correlations, b: tercile diagram at lag 4 months, c: scatter plot at lag 4 months.

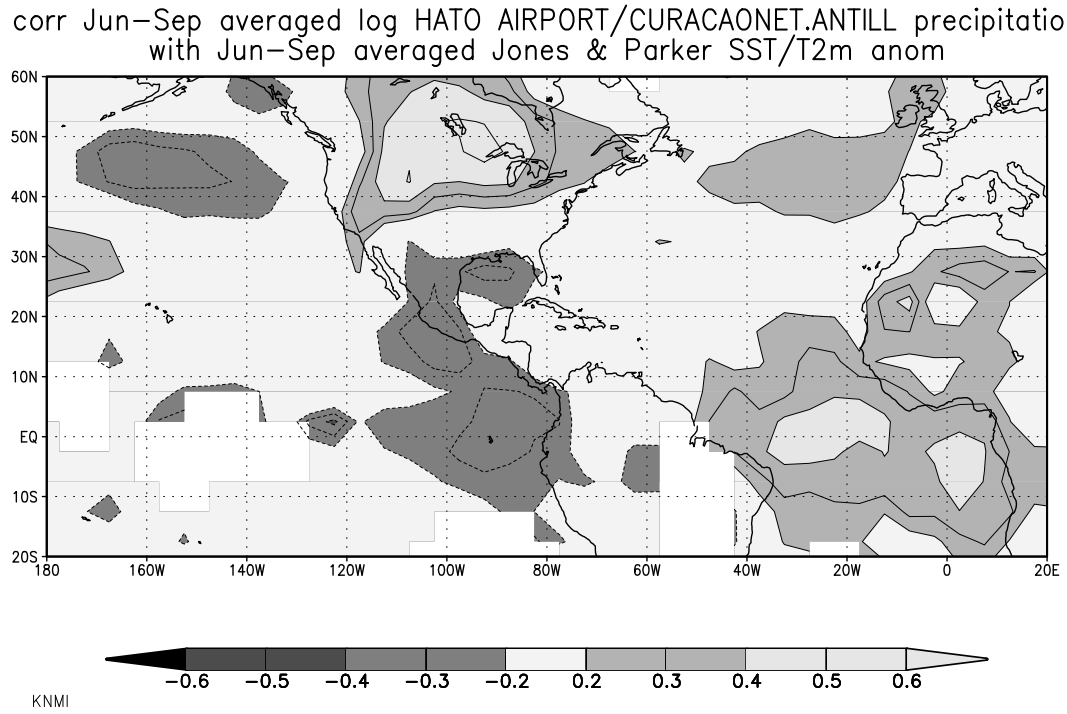

Figure 7: The correlation of the logarithm of Jun–Sep rainfall (small rains) at Hato Airport, Curaçao, with simultaneous SST/T2m.

same area that regulates the precipitation in the tropical Atlantic region (Hastenrath, 1984; Nobre and Shukla, 1996; Enfield, 1999). However, this is not a lagged relationship, so a skillful SST forecast is needed. Pointwise anomaly correlation coefficients at four months lead time of the ECMWF seasonal forecast system (Stockdale *et al.*, 1998) for this area are about $r = 0.5$. Further investigations are needed to evaluate the skill of the area average needed.

In the rest of the Caribbean the subtropical Atlantic SST index (NATL) is correlated with rainfall (Enfield, 1996). However, at Curaçao the relationship is much weaker ($r = 0.31^{+22}_{-28}$).

Finally, the Kuroshio extension area (40°–50°N, 150°–170°W) has a correlation of $r = -0.35^{+26}_{-22}$ simultaneously, and $r = -0.43^{+27}_{-23}$ at lag four months. Because there is no plausible physical link between SST in this area and rainfall on Curaçao this is treated as a coincidence.

We chose a normalized sum of the NINO3 and the tropical Atlantic indices (weights -3 and 7) as predictor; this gives a correlation of $r = 0.59^{+16}_{-21}$. The correlation is a bit larger for the index lagging the rainfall by 1–3 months, probably because the rainfall during this period is in fact concentrated in the later months (Aug–Sep). As a safer choice the NINO3 index is also considered. This index is

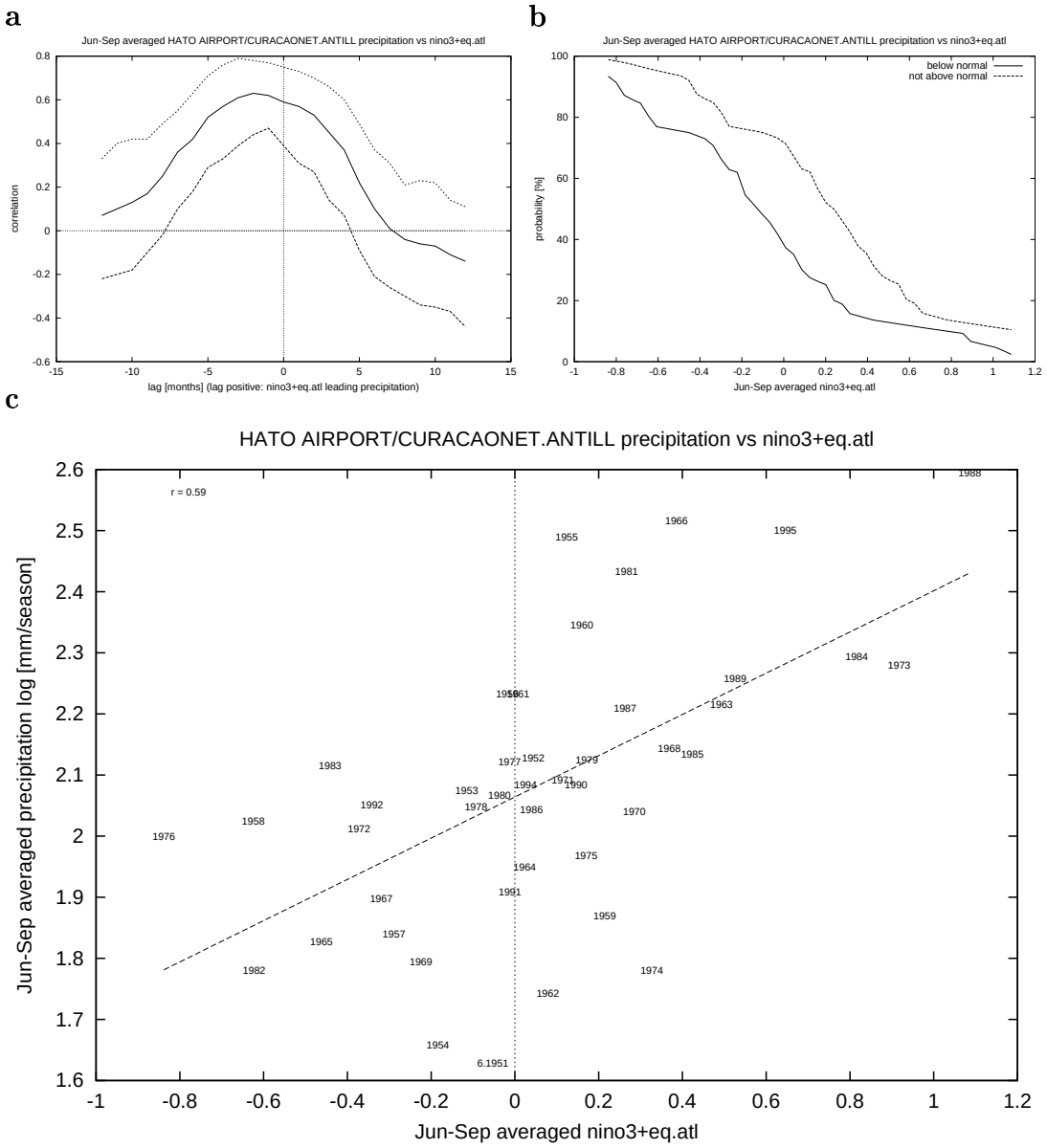

Figure 8: The correlation of the logarithm of Jun–Sep rainfall (small rains) at Hato Airport, Curaçao, with an optimized index of NINO3 and tropical Atlantic Ocean SST. a: lag correlations, b: tercile diagram, c: scatter plot. Note that forecasts of the NINO3 index and average tropical Atlantic SST are needed.

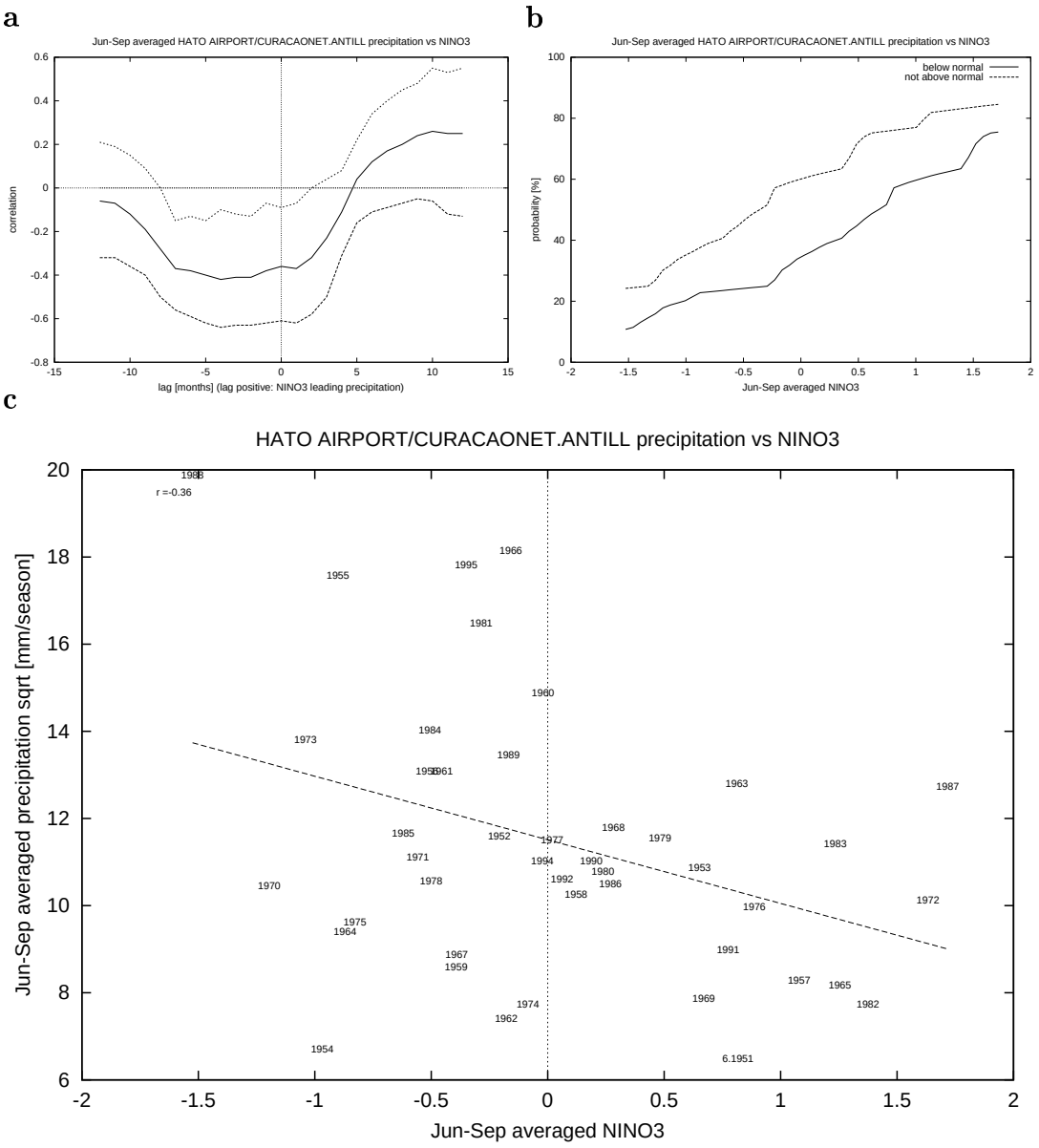

Figure 9: The correlation of the logarithm of Jun–Sep rainfall (small rains) at Hato Airport, Curaçao, with the NINO3 index. a: lag correlations, b: tercile diagram, c: scatter plot. Note that a forecast of the NINO3 index is needed.

season		predictor	lag	Hato	Willem.	Dokter.
rains	Oct–Jan	NINO3	4	-0.59^{+19}_{-15}	-0.58^{+20}_{-17}	-0.59^{+22}_{-20}
dry	Feb–May	NINO3+Pac.	4	-0.50^{+21}_{-18}	-0.52^{+19}_{-21}	-0.36^{+41}_{-40}
	–	NINO3	4	-0.31^{+23}_{-22}	-0.52^{+19}_{-20}	-0.55^{+27}_{-21}
	–	Pacific Coast	4	-0.60^{+22}_{-15}	-0.43^{+22}_{-23}	-0.13^{+51}_{-43}
small	Jun–Sep	NINO3+Eq.Atl.	0	0.59^{+16}_{-21}	0.38^{+26}_{-27}	0.25^{+29}_{-43}
	–	NINO3	0	-0.34^{+32}_{-26}	-0.52^{+24}_{-20}	-0.54^{+42}_{-27}
	–	Eq. Atlantic	0	0.50^{+19}_{-22}	0.19^{+27}_{-26}	0.05^{+37}_{-37}

Table 1: Summary of the predictors, and verification on the independent Willemstad (1894–1933) and Dokterstuin (1921–1952) precipitation data.

easier to forecast and does not involve the speculative connection to the tropical Atlantic.

3.4 Summary and verification

In Table 1 the statistical seasonal forecast models are summarized. In order to investigate the validity these have been verified on the precipitation at Willemstad, the capital, 10km south from Hato Airport on the leeward coast and Dokterstuin, 10km northwest on a small hill. The GHCN database (Vose *et al.*, 1992) has data for Willemstad from Jun 1894 to Dec 1933 with 2 missing months and for Dokterstuin from Jun 1921 to Dec 1952 with 54 missing months. This may underestimate the true association as SST measurements were less complete and had larger errors during this period. Also the Dokterstuin record overlaps with a quiet period in ENSO activity: the standard deviation of the NINO3 index during the months in which the Hato series has data is 0.85 K, for the Willemstad series it is 0.76 K and for Dokterstuin only 0.67 K.

It can be seen from Table 1 that the NINO3-based predictors verify better than the patches along the Pacific coast and the equatorial Atlantic. The values for the correlations with the Pacific coast and Equatorial Atlantic are still within each other's 2σ error bounds. The large errors for Willemstad and Dokterstuin indicate that these values are less reliable. This may be due to too few detailed SST measurements in this period, a hypothesis that is supported by the correlations obtained using the Parker SST estimates, which differ by up to 0.15. However, the possibility exists that the Equatorial Atlantic connection in the Hato series is just a coincidence, in spite of high correlation, as also suggested in Enfield (1996).

It is concluded that for all three seasons predictors can be found that have a useful correlation with station precipitation, in spite of the convective nature of the rainfall. The important rain season can be predicted with an anomaly correlation coefficient of almost 0.60 using data available at the beginning of

Station	lat.	lon.	h.	Data		Rain	Dry	Small
	°N	°W	m	1900	2000	mm	mm	mm
Aruba								
Oranjestad	12.52	70.03	-			220	44	89
Beatrix Aero	12.50	70.02	15			238	60	105
Balashi	12.48	69.98	-			236	74	112
Savaneta	12.45	69.95	-			211	32	45
Lago terrein	12.43	69.88	-			194	65	80
Curaçao								
Westpunt	12.38	69.15	13			423	80	129
Savonet	12.35	69.12	13			330	109	141
Barber	12.30	69.08	-			354	92	136
Dokterstuin	12.28	69.08	36			397	69	102
San Willibrardo	12.22	69.07	-			400	47	139
Willemstad	12.15	69.00	10			339	69	116
Hato Airport	12.20	69.00	8			320	83	143
Mar. biol. inst	12.12	68.95	15			350	71	116
St. Thomas Coll.	12.12	68.93	-			404	78	136
Suffisant	12.15	68.92	27			342	90	118
Scherpenheuvel	12.12	68.88	-			310	97	128
Santa Rosa	12.13	68.87	-			298	107	132
Nieuwpoort	12.05	68.83	-			329	72	143
Bonaire								
Rincon	12.25	68.33	28			363	68	111
Kralendijk	12.15	68.27	4			319	57	102
Tras di Montage	12.22	68.25	28			233	73	86

Table 2: All precipitation measurements of the leeward island in the GHCN v2beta database (from west to east).

these four months. The dry season still has $r \approx 0.5$ at the same lead time. For the small rains a skillful SST prediction is needed and the correlations have much larger uncertainties.

3.5 Leeward islands

In the GHCN database there are precipitation measurements from 21 stations on the leeward islands: 5 on Aruba, 13 on Curaçao and 3 on Bonaire. From these an estimate of the island-averaged precipitation can be constructed, averaging out some of the random noise from local showers. Predictions of this quantity could be useful for management of the scarce water resources on the islands, although they would overestimate the skill for an individual station. Also, these data can be used to further gauge the validity of the predictors found above.

The stations, their location, the data and some averages are given in Figure 1 and Table 2. The coordinates of Balashi, Savaneta and Willemstad have been adjusted to the position of the corresponding town on a map, as the coor-

		NINO3 (lag 4)		
	yrs	$r-2\sigma$	r	$r+2\sigma$
Aruba	21	-0.81	-0.44	-0.16
Curaçao	97	-0.71	-0.60	-0.47
Bonaire	43	-0.59	-0.42	-0.21
Leeward (all)	95	-0.73	-0.58	-0.38

Table 3: Rain season (Oct–Jan) correlations with the NINO3 index 4 months earlier.

dinates in the GHCN database were obviously wrong (in the sea).

The correlations between stations on the same island are generally $r > 0.75$, but the correlations between stations on different islands are almost always $0.60 < r < 0.80$. The differences between stations on the same island is not a strong function of the distance between them. This indicates that they can be considered independent noisy representations of the average island precipitation with a monthly normalization factor to correct for local topography. The station data $p_i(y,m)$ for stations $i = 1 \ldots N$ and years and months y, m respectively is then given by

$$p_i(y,m) = a_i(m)\Big(p_{\text{island}}(y,m) + \eta_i(y,m)\Big) \tag{1}$$

with $\eta_i(y,m)$ a white noise term. The normalization factor $a_i(m)$ is defined as the ratio of the climatology of station i with that of some reference station, $a_i(m) = \sum_y p_i(y,m) / \sum_y p_{\text{reference}}(y,m)$. The reference stations were the three airports: Beatrix for Aruba, Hato for Curaçao and Kralendijk for Bonaire. The island precipitation can then be estimated as

$$p_{\text{island}}(y,m) \approx \frac{1}{N} \sum_{i=1}^{N} p_i(y,m)/a_i(m) \tag{2}$$

with N the number of stations with data for that month. This procedure has been repeated with the three island series to obtain a composite leeward precipitation time series.

The correlations for the island estimates for the rain season are shown in Table 3. The error estimates do not take into account the varying accuracy of the points due to the number of stations included in the average. The table shows the expected result for Curaçao, $r = -0.60^{+13}_{-11}$ (note the smaller error bounds). On Aruba and Bonaire the correlation is lower. This is mainly due to 1977, which was exceptionally dry on those two islands but close to normal on Curaçao. There still is high random variability next to the predictable component.

It is concluded that the Jun–Sep NINO3 index is a good predictor for Aruba and Curaçao, and a reasonable one for Bonaire. The main mechanism in

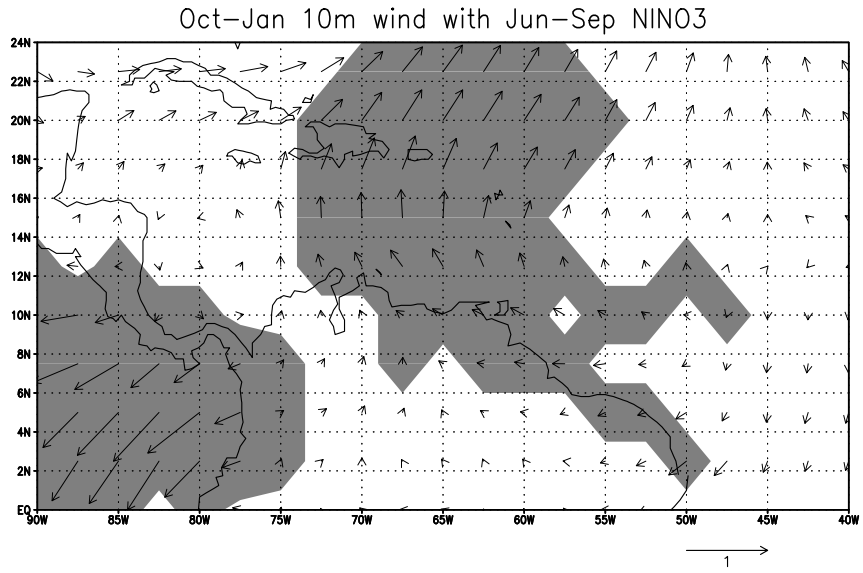

Figure 10: The regression of the NCEP/NCAR surface wind fields with the lagged NINO3 index in the rain season (Oct–Jan). Grey areas have correlations above 0.4 with horizontal divergence, vorticity at 200mb or zonal/meridional wind stress at 10m.

the NCEP/NCAR reanalysis Kalnay *et al.* (1996) winds seems to be a veering of the trade winds towards the east (Fig. 10). This will induce low-level speed and directional divergence along the coast of Venezuela (Lahey, 1958; Trewartha, 1981) and increase the sea-continent breeze circulation with its descending limb over the islands, hence suppressing precipitation on the islands.

This teleconnection forms part of a large pattern along the northern coast of South America. In Fig. 11 correlations with individual station data from the GHCN dataset with at least 40 years of data are plotted. These are large in Guyana and Surinam in the second half of the year, corresponding with the small rain season there (e.g., $r = -0.65^{+10}_{-9}$ for log Aug–Jan rain at Georgetown, Guyana, 6.80°N, 58.20°W, 134 years in 1846–1996). The same signature is seen in inland stations (e.g., $r = -0.69^{+18}_{-13}$ for log Aug–Jan rain at Santa Elena, Venezuela, 4.60°N, 61.10°W, on the border with Brazil, 53 years in 1940–1996). It seems geographically disconnected from the Oct–Jan teleconnection to the west coast of Central America and Columbia, where this time corresponds to the end of the rain season and the following dry season.

For the dry season the correlations of the individual stations are always lower than for Hato Airport, on which the relationship was tuned. The island average precipitation of Curaçao and Aruba have a correlations are about 0.4

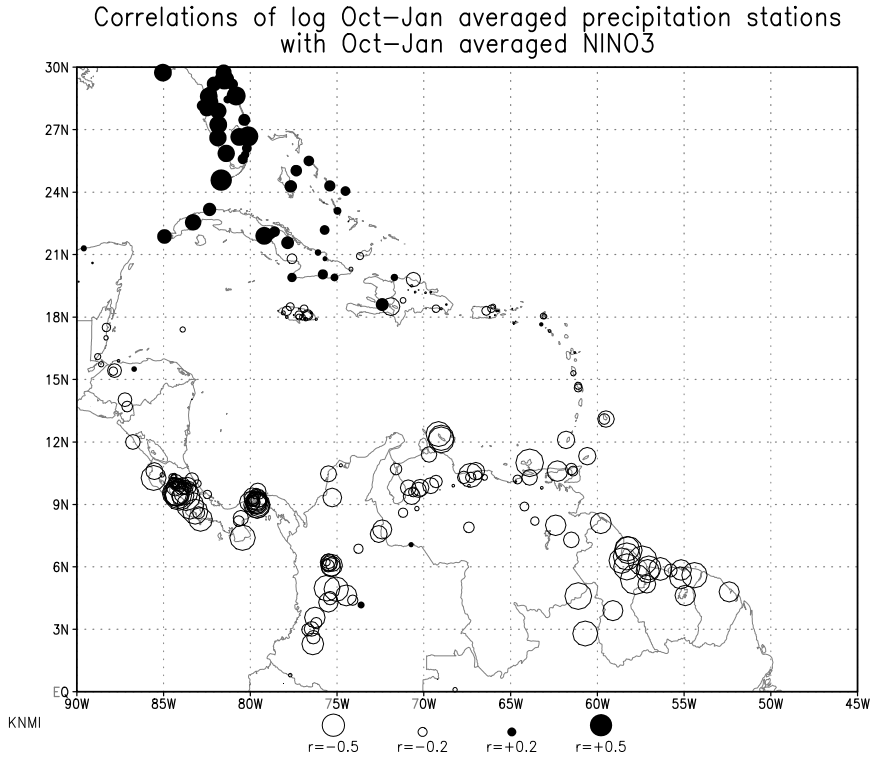

Figure 11: Oct–Jan correlations with NINO3 of log precipitation at all GHCN stations with at least 40 years of data.

		NINO3 + Pac.			NINO3		
	yrs	$r-2\sigma$	r	$r+2\sigma$	$r-2\sigma$	r	$r+2\sigma$
Aruba	24	−0.84	−0.43	0.11	−0.78	−0.37	0.19
Curaçao	95	−0.53	−0.38	−0.21	−0.52	−0.39	−0.25
1948–1996	46	−0.66	−0.52	−0.35	−0.55	−0.36	−0.13
Bonaire	49	−0.48	−0.21	0.01	−0.58	−0.37	−0.16
1948–1985	25	−0.73	−0.44	−0.13	−0.68	−0.39	−0.14
Leeward (all)	95	−0.52	−0.39	−0.22	−0.54	−0.40	−0.25
1948–1996	46	−0.55	−0.51	−0.30	−0.57	−0.37	−0.14

Table 4: Dry season correlations with the weighted sum of NINO3 index and Pacific Coast SST 4 months earlier.

		Eq.Atl.			NINO3		
	yrs	$r-2\sigma$	r	$r+2\sigma$	$r-2\sigma$	r	$r+2\sigma$
Aruba	24	−0.30	0.17	0.55	−0.76	−0.49	−0.17
Curaçao	98	0.01	0.21	0.41	−0.63	−0.45	−0.23
1948–1996	46	0.16	0.43	0.63	−0.73	−0.48	−0.17
Bonaire	50	−0.21	0.08	0.36	−0.60	−0.42	−0.17
1948–1985	25	−0.10	0.26	0.55	−0.63	−0.38	0.00
Leeward (all)	98	−0.02	0.18	0.39	−0.62	−0.45	−0.23
1948–1996	46	0.12	0.37	0.58	−0.70	−0.45	−0.16

Table 5: Small rain season (Jun–Sep) correlations with Equatorial Atlantic SST and the NINO3 index.

with the predictor, the linear combination of NINO3 and SST along the pacific coast of Central America. If the hypothesis of better SST measurements in the second half of the previous century is correct the correlations would be higher after 1948. This is indeed the case, so these values are likely to be a better estimate of the true correlation.

It is concluded that the precipitation in the dry season can be predicted with some skill, $r = 0.4$ to 0.5, using a combination of the NINO3 index and SST along the pacific coast of Central America. The errors on the relationship are rather large: the older SST data are uncertain, and the period afterwards has too few years to compute it more accurately. In spite of the difference in mean precipitation the main mechanism seems to be the same as in the rain season.

The lagged connections with ENSO and with Pacific Coast SST extend to the east to Isla Margarita ($r = -0.38$ and -0.63 respectively at La Asuncion, 11.00°N, 63.90°W, 1949–1989 with 23 missing months). Both also show up in west-Venezuelan and north-Columbian stations, shifted to Dec–Mar together with the dry season ($r = -0.4$ to -0.6, not shown).

Finally we turn again to the small rains season (Jun–Sep). The correlations with the equatorial Atlantic SST is weak or absent in almost all stations except Hato Airport, on which it was tuned. This may in part be due to poorer SST measurements, but a more likely explanation is that the relationship is much weaker than the Hato data indicated. The estimate of average precipitation on all three leeward islands has a correlation with equatorial Atlantic SST of $r = 0.18$ only, compatible with zero at the 95% confidence level (Table 5). In contrast, the link with the simultaneous NINO3 index is stronger in the data of the other stations and therefore the averages. As this index is much easier to predict also, it is chosen as predictor for the small rains, again with a skill of $r = 0.4$–0.5.

As in the other periods the backing of the trade wind will result in reduction of the descending limb of the sea-continental breeze and speed and directional

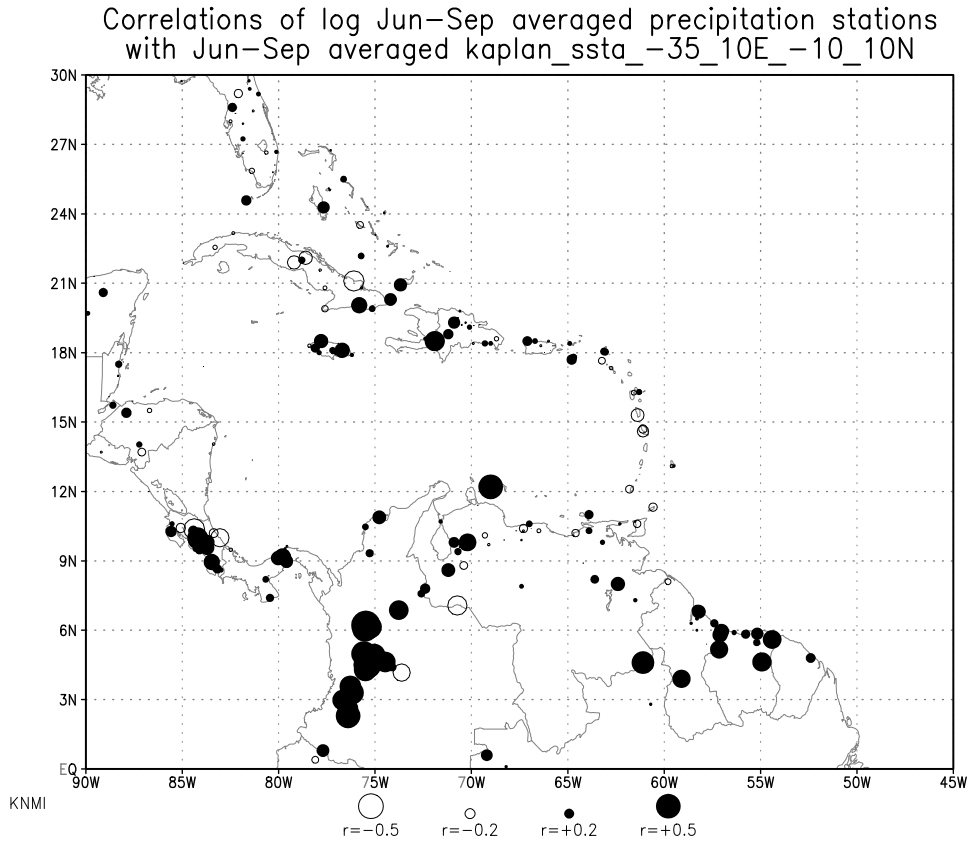

Figure 12: Jun–Sep correlations with equatorial Atlantic SST of log precipitation at all GHCN stations with at least 40 years of data.

divergence. During this period the wind speed west of the islands are normally higher then over the islands resulting in a low-level speed divergence over the islands. Therefore a reduction of the trade winds west of the islands will reduce the low level divergence. Finally, there is a strong connection to low-level vertical shear in this season. High shear will reduce the vertical development of a convective cloud.

The ENSO connection shows large correlations everywhere in northern South America and along the Pacific coast of Costa Rica and Panama. Many stations in Jamaica also show this teleconnection. Boreal summer is the main rain season in much of this area, and apparently very sensitive to condition in the Pacific Ocean in this off-season for El Niño (the standard deviation of the NINO3 index is 25% lower than in the boreal winter).

Although the analysis of independent measurements on the Dutch Antilles had led us to the conclusion that the correlation with the equatorial Atlantic

Ocean in the Hato series was probably spurious, this signal shows up in a coherent band extending to Colombia (Figure 12). Further investigation is needed to establish the reality of this teleconnection.

4 Conclusions

The location of the Netherlands Antilles islands of Aruba, Bonaire and Curaçao off the northern coast of South America not only leads to their semi-arid climate, but also to good seasonal predictability of the precipitation, which is very sensitive to changes in the circulation. A statistical analysis of station data on the islands shows that the logarithm of precipitation during the main rain season (Oct–Jan) is linearly correlated with the strength of El Niño four months earlier with a correlation coefficient $r \approx -0.6$. La Niña's have invariably been followed by wet seasons, whereas most El Niño's have caused droughts. The lagged relationship implies a seasonal forecast at the beginning of the season can be made using only observations of the NINO3 index. Longer lead times require the use of ENSO forecasts.

The dry season (Feb–May) is also correlated to ENSO. There is also a statistical connection to the SST off the Pacific coast of Central America. A lag of four months gives a correlation coefficient $r \approx -0.5$ to a combination of these two predictors. The verification of the Pacific coast SST teleconnection on independent older data is somewhat problematic, probably due to the quality of SST measurements before 1950. Finally, the small rain season (Jun–Sep) is correlated with simultaneous NINO3 at $r \approx -0.45$. A skillful ENSO forecast is therefore needed to make predictions. There also seems to be a connection with tropical Atlantic SST. This teleconnection cannot be verified with independent older data, but reappears again in station data in northwestern South America.

The statistical seasonal forecasts are also valid for other islands in the Caribbean dry zone, such as Isla Margarita. The boreal summer connection to ENSO extends along the whole north coast of South America, where the secondary rain season often falls in these months. The dry season teleconnection to Pacific coastal SST extends to coastal Colombia.

Acknowledgements All figures except Fig. 10 were obtained from the KNMI Climate Explorer web application (van Oldenborgh and Burgers, 2001). Albert Martis would like to thank KNMI for hospitality.

References

Enfield, D. B. 1996. 'Relationships of inter-American rainfall to tropical Atlantic and Pacific SST variability', *Geophys. Res. Lett.*, **23,** 3305–3308.

Enfield, D. B. 1999. 'How ubiquitous is the dipole relationship in the tropical Atlantic sea surface temperatures?', *J. Geophys. Res.*, **104,** 7841–7848.

Enfield, D. B. and Alfaro, E. J. 1999. 'The dependance of Caribbean rainfall on the interaction of the tropical Atlantic and Pacific oceans', *J. Climate,* **12,** 2093–2103.

Giannini, A., Kushnir, Y., and Cane, M. A. 2000. 'Interannual variability of Caribbean rainfall, ENSO, and the Atlantic Ocean', *J. Climate,* **13,** 297–311.

Hastenrath, S. 1984. 'Interannual variability and annual cycle: mechanisms of circulation and climate in the Tropical Atlantic sector', *Mon. Wea. Rev.*, **112,** 1097–1107.

Hastenrath, S. 1995. 'Recent advances in tropical climate prediction', *J. Climate,* **8,** 1519–1532.

Ji, M., Leetmaa, A., and Kousky, V. E. 1996. 'Coupled model predictions of ENSO during the 1980s and 1990s at the National Centers for Environmental Prediction', *J. Climate,* **9,** 3105–3120. Forecasts are under www.cdc.noaa.gov.

Jones, P. D. 1994. 'Hemispheric surface air temperature variations: a reanalysis and an update to 1993', *J. Climate,* **7,** 1794–1802. Data are available from www.cru.uea.ac.uk/cru/data/temperat.htm.

Kalnay, E., Kanamitsu, M., Kistler, R., Collins, W., Deaver, D., Gandin, L., Iredell, M., Saha, S., White, G., Woollen, J., Zhu, Y., Leetma, A., Reynolds, R., Chelliah, M., Ebisuzaki, W., Higgens, W., Janowiak, J., Mo, K. C., Ropelewski, C., Wang, J., and Jenne, R. 1996. 'The ncep/ncar 40-year reanalysis project', *Bull. Amer. Met. Soc.,* **77,** 437–471.

Kaplan, A., Cane, M. A., Kushnir, Y., Clement, A. C., Blumenthal, M. B., and Rajagopalan, B. 1998. 'Analyses of global sea surface temperature 1856–1991', *J. Geophys. Res.,* **103,** 18567–18589. Data are available from ingrid.ldgo.columbia.edu.

Kiladis, G. N. and Diaz, H. F. 1989. 'Global climatic anomalies associated with extremes in the southern oscillation', *J. Climate,* **2,** 1069–1090.

Lahey, J. F. 1958. 'On the origin of the dry climate in the northern South American and the southern Caribbean', Scientific Report 10 University of Wisconsin.

Nobre, P. and Shukla, J. 1996. 'Variations of sea surface temperature, wind stress, and rainfall over the tropical Atlantic and south America', *J. Climate,* **9,** 2464–2479.

Parker, D. E., Folland, C. K., and Jackson, M. 1995. 'Marine surface temperature: observed variations and data requirements', *Climatic Change,* **31,** 559–600.

Parker, D. E., Jones, P. D., Bevan, A., and Folland, C. K. 1994. 'Interdecadal changes of surface temperature since the late 19th century', *J. Geophys. Res.,* **99,** 14373–14399. Data are available from www.cru.uea.ac.uk/cru/data/temperat.htm.

Reynolds, R. W. and Smith, T. M. 1994. 'Improved global sea surface analyses using optimum interpolation', *J. Climate,* **7,** 929–948. NINO indices are available from the Climate Prediction Center at www.cpc.noaa.gov/data/indices/.

Ropelewski, C. F. and Halpert, M. S. 1987. 'Global and regional scale precipitation patterns associated with the El Niño/Southern Oscillation', *Mon. Wea. Rev.,* **115,** 1606–1626.

Stockdale, T. N., Anderson, D. L. T., Alves, J. O. S., and Balmaseda, M. A. 1998. 'Global seasonal rainfall forecasts using a coupled ocean–atmosphere model', *Nature,* **392,** 370–373.

Trewartha, G. T. 1981. *The Earth's Problem Climate* University of Wisconsin.

van Oldenborgh, G. J. and Burgers, G. 2001. 'The effects of El Niño on precipitation and temperature, an update', *KNMI preprint 2001-07,*. The KNMI Climate Explorer is available at climexp.knmi.nl.

Vose, R. S., Schmoyer, R. L., Steurer, P. M., Peterson, T. C., Heim, R., Karl, T. R., and Eischeid, J. K. 1992. 'The global historical climatology network: Long-term monthly temperature, precipitation, sea level pressure, and station pressure data', Technical Report NDP-041 Carbon Dioxide Information Analysis Center, Oak Ridge National Laboratory Oak Ridge, Tennessee, U.S.A.

Wilks, D. S. 1995. *Statistical Methods in the Atmospheric Sciences: an Introduction* Academic Press 464pp.